Quaternary Research 71 (2009) 426–436

Contents lists available at ScienceDirect

Quaternary Research

journal homepage: www.elsevier.com/locate/yqres

Using remote sensing to quantify aeolian transport and estimate the age of the terminal dune field Dunas Pampa Blanca in southern Peru

Ralf Hesse *

Department of Geography, Friedrich Schiller University Jena, 07740 Jena, Germany

ARTICLE INFO

Article history:
Received 19 April 2008
Available online 18 March 2009

Keywords:
Peru
Aeolian transport
Dunes
Paleoclimate
Remote sensing

ABSTRACT

Aeolian dunes are widely used to reconstruct paleoenvironmental conditions. However, terminal dune fields (ergs) in the coastal desert of southern Peru – where information regarding Quaternary paleoenvironmental conditions is very limited – have until now not been used for paleoenvironmental reconstructions and the time depth of their accumulation is unknown. Here, different estimates are derived to constrain the time depth recorded in the Dunas Pampa Blanca, a terminal dune field in coastal southern Peru. Dune field age is calculated using the volume of the Dunas Pampa Blanca and (i) recent aeolian transport rate in migrating transverse dunes feeding the Dunas Pampa Blanca (derived from digital processing of sequential Landsat and Quickbird images) and (ii) limitations posed by recent fluvial sediment supply to the source of aeolian transport. The resulting maximum age estimate of 70 ± 8 ka (from aeolian transport) compares with a minimum age estimate of 4–75 ka (from sediment supply). However, a minimum age estimate of 110–450 ka is deduced from the tectonic and topographic evolution of the region. This discrepancy contradicts the hypothesis of late Quaternary stability in the Peruvian coastal desert and indicates that recent conditions of aeolian sediment supply and transport are not representative for the late Quaternary.

Introduction

On the coast of Peru and northern Chile, hyperarid conditions are thought to have prevailed since the Miocene (Clarke, 2006; Rech et al., 2006). However, while a variety of proxy data and paleoenvironmental reconstructions are available for the Andean highlands (Macharé et al., 1990; Grosjean et al., 2003), the climatic history of the coastal desert is largely unknown. Although the factors underlying the aridity have persisted at least since the Miocene, fluvial and debris flow sediments as well as stacked terraces in local catchments are evidence for deviations from the prevailing conditions, either through short-term, episodic El Niño events or long-term climatic changes (e.g. Noller, 1993; Sébrier and Macharé, 1980). Timing, duration and intensity of Quaternary climatic changes in the coastal desert are not well understood and the question as to what extent present conditions can be considered representative for the Quaternary remains unsolved.

In general, paleoenvironmental reconstructions in the coastal desert of Peru are hampered by a paucity of well-datable, high-resolution records outside of the allogenic river valleys which are influenced by both coastal and highland climates. Large sand dunes may offer such records. However, investigations of dunes in Peru have until now focused on the morphology and dynamics of migrating barchans (Finkel, 1959; Lettau and Lettau 1969; Gay, 1999). While aeolian sediments have been recognised for their potential as geoarchives elsewhere (e.g. Wasson et al., 1983; Besler, 2002; Singhvi and Kar, 2004; Mahan et al., 2007), their potential for paleoenvironmental reconstructions has so far received little attention in this region. In particular, even the age of Peruvian dunes is unknown.

The aim of this paper is to investigate the potential time depth recorded in the southern Peruvian terminal dune field Dunas Pampa Blanca. Digital elevation models (DEM) and satellite images are used to determine the volume of sediment stored in the Dunas Pampa Blanca as well as the recent rate of aeolian sediment flux to these dunes. It is known from several studies that in other parts of the world aeolian activity has varied throughout the Quaternary (e.g. Argentina: Zárate and Blasi, 1993; Australia: McGowen et al., 2008; Canada: Wolfe et al., 2007; China: Wang et al., 2004; India: Singhvi and Kar, 2004; Oman: Radies et al., 2004; USA: Forman et al., 2001; Lancaster, 1994a). However, in the light of the high age of the Peruvian coastal desert (Alpers and Brimhall, 1988; Arancibia et al., 2005; Rech et al., 2006; Clarke, 2006), its exceptional climatic stability (Weischet, 1966, 1996) and the paucity of paleoenvironmental data, variations in aeolian activity cannot be taken for granted. Therefore, one objective of this paper is to assess whether or not the present conditions could hypothetically be considered representative for the Quaternary. To this end, age estimates for the Dunas Pampa Blanca based on recent conditions of aeolian sediment supply and transport and on the potential age derived from the tectonic history of the region are compared.

* Fax: +49 3641 948812.
E-mail address: Ralf.Hesse@uni-jena.de.

0033-5894/$ – see front matter
doi:10.1016/j.yqres.2009.02.002

Regional setting and climatic conditions

The study region (Figs. 1 and 2) is located in the Peruvian–Chilean coastal desert, the Chilean portion of which is known as the Atacama. This desert extends for 3200 km from Talara in northern Peru to Santiago de Chile (Gay, 1962). Aeolian transport corridors of migrating barchan and transverse dunes are common in the coastal desert of Peru. However, large terminal dune fields (ergs) at the end of these corridors occur mainly in the study region between Pisco (13.7°S) and Tanaca (15.7°S). Here, uplift driven by the oceanic Nazca Ridge has led to a widening of the desert lowlands and to the creation of a coastal mountain range (Cordillera de la Costa) west of the Andes (Hsu, 1992). The close correspondence between the presence of the Cordillera de la Costa and the accumulation of large terminal dune fields indicates a strong topographic influence on the genesis of these dune fields (Gay, 2005). In the present study, the Dunas Pampa Blanca, a moderately sized (60 km^2) erg in southern Peru, were chosen for investigations regarding the rate and age of aeolian accumulation.

The Dunas Pampa Blanca are situated on the western margin of the Pre-Andean Basin at 14.53–14.64°S, 75.31–75.38°W in the centre of the segment of the Peruvian coast in which the Cordillera de la Costa is present. They are located approximately 40–50 km inland from the coast in the lee of Cerro Machocoyungo (1002 m), one of the highest mountains in the Cordillera de la Costa. The main fault separating the uplifting Cordillera de la Costa from the Pre-Andean Basin runs perpendicular to the direction of prevailing wind and sand transport. Aeolian sediment is supplied by a 3–12 km wide aeolian transport corridor crossing the Pampa Coyungo and Cerro Machocoyungo. The source of aeolian sediment is the coastline of the Pacific Ocean 8–15 km north of the mouth of the Rio Grande de Nazca. Sediment supply is modulated by fluvial suspended sediment delivery of the Rio Grande (Gay, 1999). The aeolian transport corridor widens as it crosses Cerro Machocoyungo. In the lee of this obstacle, winds, and consequently sand transport, converge towards the Dunas Pampa Blanca where most if not all sand accumulates. Beyond the Dunas Pampa Blanca, no migrating dunes are present. In the Late Intermediate Period archaeological site Ciudad Perdida de Huayuri, which is located

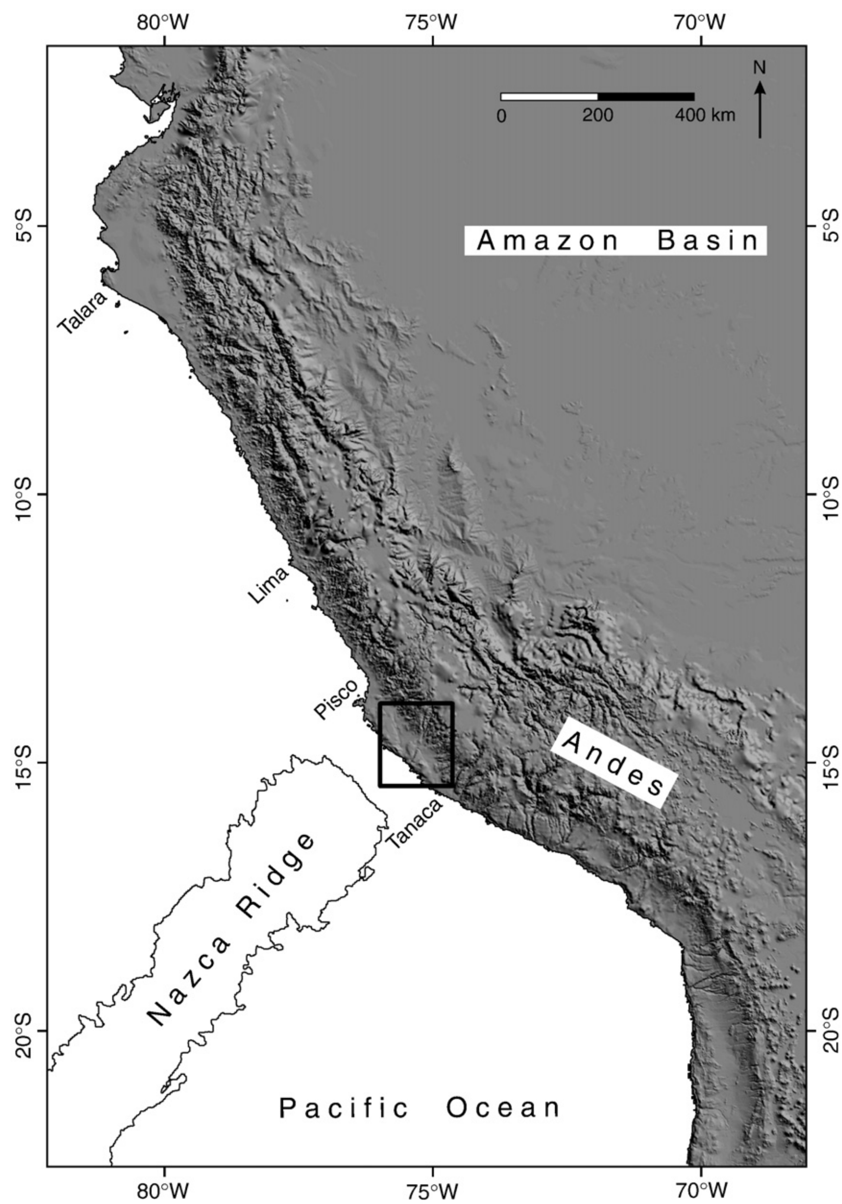

Figure 1. Relief map of western South America showing the location of the research area (enlarged in Fig. 2). Nazca Ridge is shown as 4000 m isobath.

https://doi.org/10.1016/j.yqres.2009.02.002 Published online by Cambridge University Press

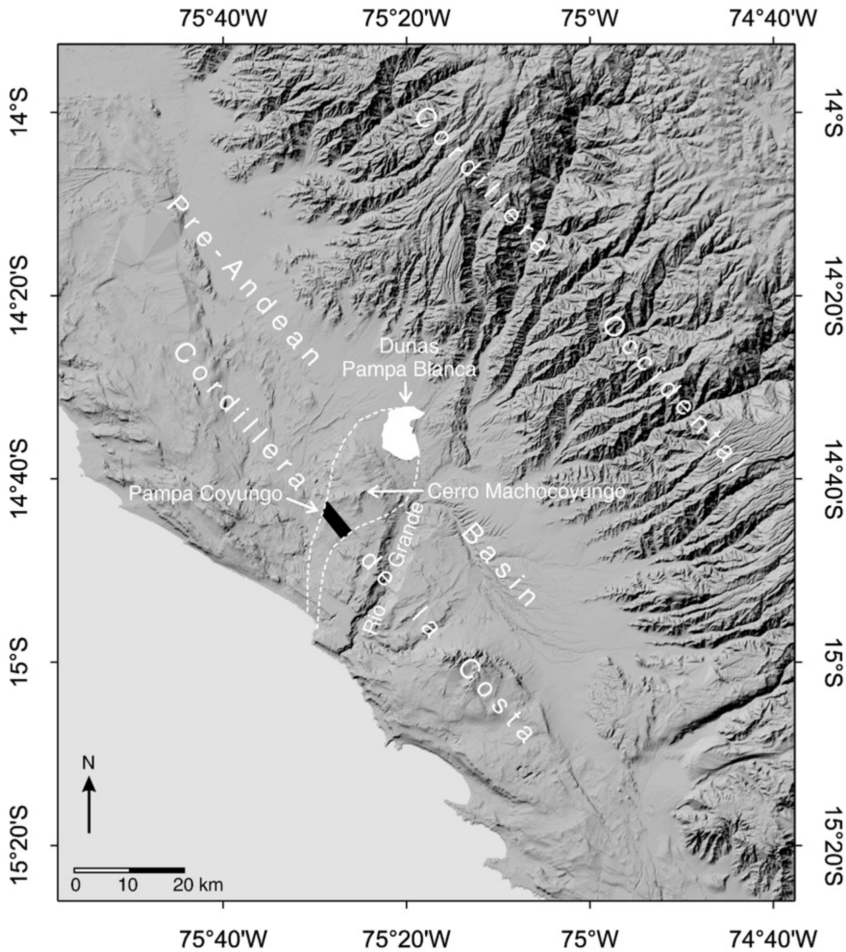

Figure 2. SRTM relief map of the research area indicating the location of the Dunas Pampa Blanca (white), the corresponding aeolian transport corridor (within dashed limits) and the transect in which dune migration was quantified (black).

~4 km east of the north-eastern margin of the Dunas Pampa Blanca, only a few centimetres of aeolian sediment have accumulated in the ≥600 a since the abandonment of the site (before AD 1400, cf. Unkel, 2006). The seasonal, allogenic Rio Santa Cruz which runs in a north-south direction east of the eastern margin of the Dunas Pampa Blanca has an average discharge of 5.3×10^6 m^3 a^{-1} (data for the period 1975–2007, Junta de Usuarios Palpa, 2007). This implies a potential to remove aeolian sand deposited in the river channel. However, for much of the stretch of the river along the Dunas Pampa Blanca the dunes do not reach down to the valley floor from the bajada terrace. In the southern part of the dune field, where dunes are present close to the Rio Santa Cruz, they migrate parallel to the river.

Present-day climatic conditions in the coastal desert are hyperarid. At the station Palpa, mean annual precipitation is less than 10 mm a^{-1}, potential evaporation is 1648 mm a^{-1} and mean monthly temperatures range between 16 and 26°C (ONERN, 1971). Measurable precipitation occurs only at irregular intervals of several years (Weischet, 1966; Oberlander, 1994). While El Niño events regularly lead to strong precipitation and geomorphic impacts in northern Peru, this influence is less pronounced in southern Peru (e.g. Barber and Chavez, 1983; Cane, 1983; Caviedes, 1984; Noller, 1993).

Climatic conditions in coastal Peru are controlled by the South-East Pacific Anticyclone (SEPA) (Messerli et al., 1992; Messerli et al., 1993). Meridional position and strength of the SEPA are stabilised and reinforced by the Andes which also block moisture transport from the Amazon Basin (Weischet, 1966). Descending air in the SEPA combined with the thermal effect of marine upwelling causes a very stable inversion in the lower troposphere (Gay, 1962; Weischet, 1966; Prohaska, 1973; de Abreu and Bannon, 1993) which in turn inhibits convection and convective precipitation over the subtropical south-east Pacific and adjacent land areas (Caviedes, 1973; Weischet, 1966). Sea–land temperature gradients cause a diversion of the SEPA-related trade winds: near-surface air movement over the coast is dominated by sea winds (de Abreu and Bannon, 1993 for Lima; Gay, 1962, 1999 and 2005 for southern Peru).

The initiation of arid conditions along the west coast of South America due to the uplift of the Andes as a moisture barrier is widely accepted (Macharé et al., 1990; Houston and Hartley, 2003). Generally arid conditions have therefore been in place for millions of years (e.g. Oberlander, 1994; Clarke, 2006). Uplift of the Andes during the Tertiary led to a stabilisation of the SEPA and the creation of rain-shadow conditions. Arid conditions in the Atacama have persisted at least since the Late Eocene and hyperarid conditions since the Middle to Late Miocene (Alpers and Brimhall, 1988; Arancibia et al., 2005; Rech et al., 2006). During the Quaternary, fundamental climatic changes in the coastal desert should not be expected as the height of the Peruvian Andes did not change significantly (Macharé et al., 1990). However, despite generally hyperarid conditions at least since the Miocene, substantial precipitation must have occurred to deposit and dissect the ubiquitous large alluvial fans in the coastal desert (Evenstar et al., 2005; Macharé et al., 1990; Sébrier and Macharé, 1980). It is not known to what extent these changes in moisture were linked with changes in the wind climate and may have influenced aeolian processes and landforms.

Data and methods

Data

The data used in this study are digital elevation models (DEM) based on SRTM (Shuttle Radar Topography Mission, NASA, 2006a) and ASTER (Advanced Spaceborne Thermal Emission and Reflection Radiometer, NASA, 2006b) as well as three Landsat images (Landsat MSS of 30 April 1974: GLCF, 2004; Landsat TM of 23 April 1990; Landsat ETM of 26 April 2000: NASA, 2005) and a Quickbird image of 15 March 2003 (DigitalGlobe, 2003). Landsat MSS band 4, Landsat TM and ETM band 7 as well as Quickbird band 3 were used. As all images

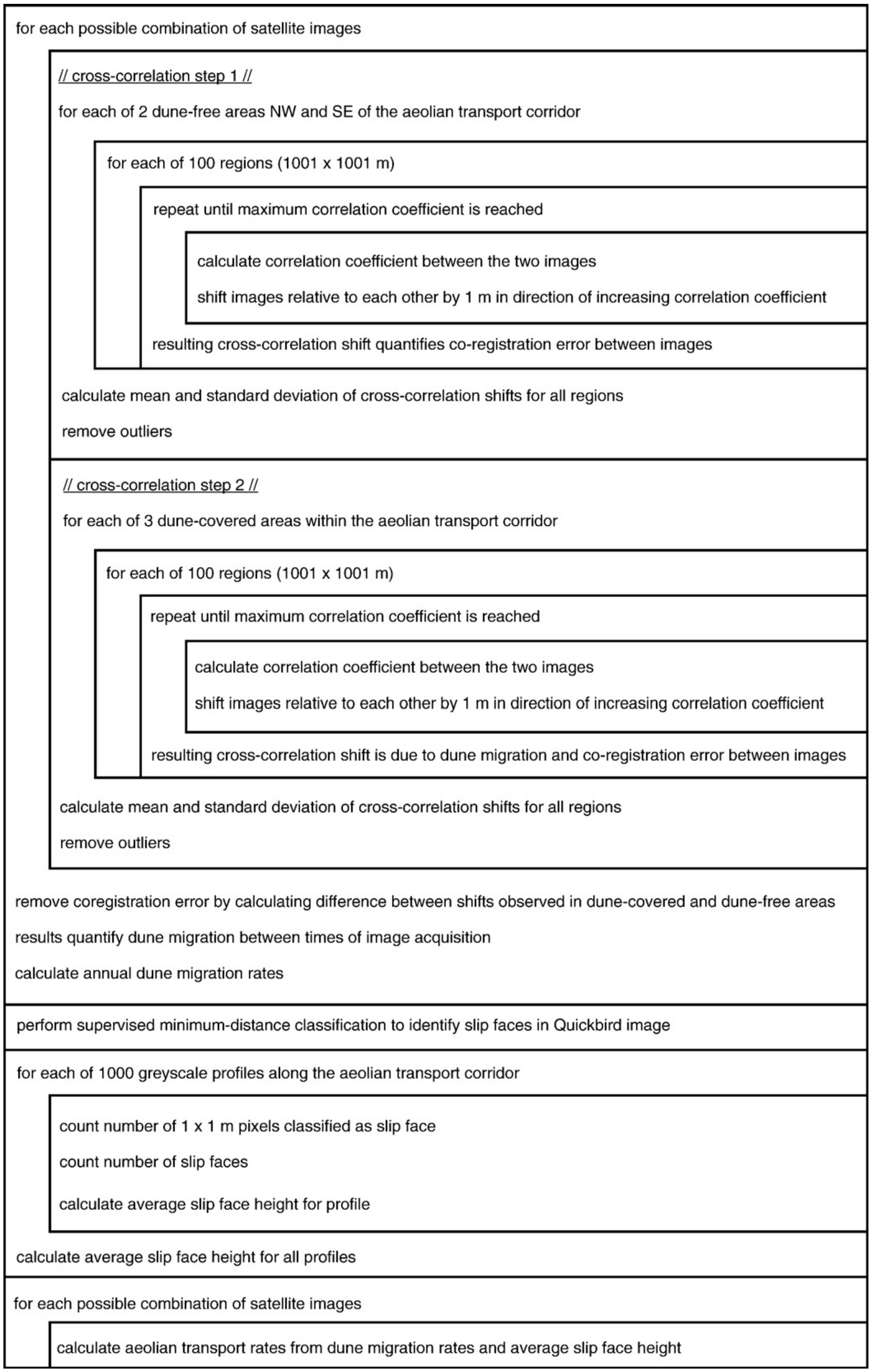

Figure 3. Pseudocode structure illustrating the calculation process to derive aeolian transport rates (see text).

Figure 4. Landsat image taken in 2000 (NASA, 2005) of the investigated segment of the aeolian transport corridor. White arrows indicate direction of dune migration; white rectangle shows transect for which average dune height was determined.

were acquired at ca. 11:00 a.m. between mid-March and late April, they were recorded at almost identical sun azimuth and elevation angles. The differences in pixel brightness are primarily due to differences in reflectance and secondarily due to sun incidence angle. Given the high sun elevation angle at the times of image acquisition and maximum dune slopes of 33° (angle of repose; cf. Bourke et al., 2006), shade is not an issue. The slip faces in the study area are characterised by very high reflectance. Therefore – given the shape of the dunes – pixel brightness values allow the distinction of slip faces under a wide range of incidence angles. Cloud cover was minimal in all images and care was taken to avoid cloud-covered areas in all processing steps described below.

Calculation of terminal dune field volume

To derive the volume of aeolian sediment stored in the Dunas Pampa Blanca, the basal topography of the dune field was interpolated from elevations of the surrounding terrain. As the dune field lies on a large bajada with very limited topographic roughness, this approach can be expected to deliver reliable results. Basal topography of the Dunas Pampa Blanca was interpolated by manually masking the dune field along its perimeter and using the interpolation algorithm in ENVI. Sand thickness was then calculated by subtracting the basal topography values from the original DEM values. Subsequently, dune field volume was calculated by spatially integrating the derived sand thicknesses. Basal topography interpolation, sand thickness calculation and volume calculation were performed for both the ASTER and the SRTM DEM. Performance of DEM generation using optical photogrammetry may have been limited by the large, featureless areas within the dune fields while SAR relies on radar backscatter which is poor for dry sand (Lewis et al., 1998). However, while both DEMs are thus based on methods which are not ideally suited for large, dry sand dunes, the comparison of the results allows an estimation of error.

Quantification of aeolian transport

Aeolian sediment flux towards the Dunas Pampa Blanca was quantified by observing the migration of transverse dunes in the aeolian transport corridor. Shifts in dune position between three Landsat images taken in April 1974 (GLCF, 2004), April 1990 and April 2000 (NASA, 2005) and a Quickbird image taken in March 2003 (DigitalGlobe, 2003) were used to determine the migration rate. The Quickbird image (DigitalGlobe, 2003) was further used to determine average dune height. Figure 3 summarises the data processing described below.

Because the spatial resolution of Landsat images (79 m for Landsat MSS, 30 m for Landsat TM, 15 m for Landsat ETM) is not sufficient to accurately measure the displacement of individual point targets, a cross-correlation approach (Wernstedt, 1989) was applied to measure dune displacement. All satellite images were resampled to a resolution of 1×1 m using bicubic resampling. Because a very high number of data points (200 and 300 regions with ~10^6 data points each) all experiencing similar positional shifts were sampled, the cross-correlation approach allows sub-pixel resolution with regard to the original data. Possible co-registration errors had to be taken into account because the accuracy of co-registration between the individual satellite images was not known. Therefore, two steps were necessary to quantify dune displacement. First, co-registration errors between the satellite images were determined using two areas outside (north-west and south-east) of the aeolian transport corridor, i.e. covering dune-free land surface. In each of the two areas and for each combination of satellite images, cross-correlation between 100 pairs of 1001×1001 m regions was calculated using

$$r = \frac{\frac{1}{1001^2} \cdot \sum_{x=-500}^{500} \sum_{y=-500}^{500} \left((a_{x,y} - \bar{a}) \cdot \left(b_{x,y} - \bar{b} \right) \right)}{\sqrt{\frac{1}{1001^2} \cdot \sum_{x=-500}^{500} \sum_{y=-500}^{500} (a_{x,y} - \bar{a})^2} \cdot \sqrt{\frac{1}{1001^2} \cdot \sum_{x=-500}^{500} \sum_{y=-500}^{500} \left(b_{x,y} - \bar{b} \right)^2}} \quad (1)$$

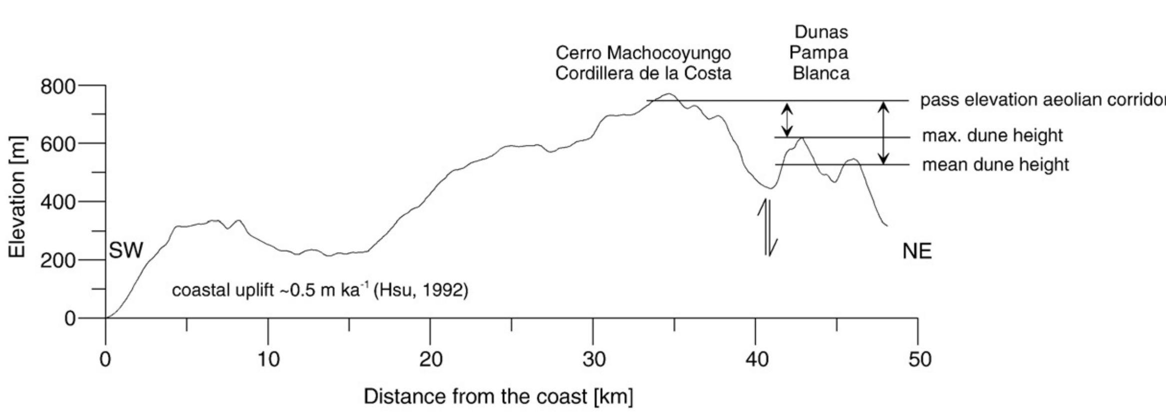

Figure 5. Elevation profile along the aeolian transport corridor indicating the wind shadow position of the Dunas Pampa Blanca behind the uplifting Cordillera de La Costa from which the antiquity of topographic conditions favourable for terminal dune field accumulation was estimated.

https://doi.org/10.1016/j.yqres.2009.02.002 Published online by Cambridge University Press

where r is the correlation coefficient, x and y are pixel coordinates relative to the centre coordinates of the 1001 × 1001 m regions, $a_{x,y}$ and $b_{x,y}$ are pixel greyscale values of the two satellite images and $\bar{a}$ and $\bar{b}$ are the mean pixel greyscale values over the 1001 × 1001 m regions. The position of the maximum correlation coefficient was found using a gradient approach, i.e. the two paired regions were shifted relative to one another by 1 m in the direction of increasing correlation coefficient until a maximum was reached. No a-priori limits were applied to the relative shifts. The resulting positional shifts quantify the co-registration shifts between the individual satellite images. Outliers exceeding a threshold distance of three standard deviations from the mean were removed (Sun, 2006).

In the second step, cross-correlation shifts for areas within the aeolian transport corridor (i.e. in areas of migrating transverse dunes) were determined. Calculations were performed as described above, i.e. for each of three areas within the aeolian transport corridor and each combination of satellite images, cross-correlation between 100 pairs of 1001 × 1001 m regions was calculated. The gradient approach as described above was used and outliers were removed as described above. Because in this case the cross-correlation approach was applied in areas of continuous dune cover, the resulting shifts quantify the migration of the dunes, albeit biased by co-registration shifts between the respective satellite images. Dune migration rates are then calculated by subtracting the co-registration errors derived in the first step.

Dune crest heights were determined within a transect (Fig. 4) spanning the entire width of the aeolian transport corridor perpendicular to the direction of dune migration. Dune slip faces were identified by applying a supervised minimum distance classification to the Quickbird image (DigitalGlobe, 2003; resampled to a resolution of 1 × 1 m). Within the transect, 1000 narrowly spaced greyscale profiles were extracted in the direction of dune migration. For each greyscale profile, the number of pixels classified as slip face as well as the number of slip faces were counted. Average dune slip face length L was calculated as

$$L = \frac{1}{1000} \cdot \sum_{p=1}^{1000} \frac{S_p}{N_p \cdot \sin\alpha} \tag{2}$$

where p is the greyscale profile number, S_p is the number of 1 × 1 m slip face pixels in profile p, N_p is the number of slip faces in profile p and α is the angle between North and the direction of the profile. Assuming an angle of repose of 33° (Bourke et al., 2006), average slip face height H was calculated as

$$H = \tan(33^\circ) \cdot L. \tag{3}$$

While the total height of the transverse dunes is mostly larger than slip face height H (i.e., the base is not exposed between dunes), slip face height is assumed to represent the height of the migrating dune body. Aeolian transport rate T was calculated from dune migration rate R and aeolian transport corridor width W as

$$T = H \cdot W \cdot R. \tag{4}$$

Error propagation was taken into account in all calculation steps. Results are given as 99% confidence ranges (±), and standard deviations (SD) are given as additional information.

Limitation of sediment supply

Sediment supply calculations based on fluvial suspended sediment delivered to the littoral by the Rio Grande de Nazca were performed to derive additional age estimates. Gay (1999) and Moseley et al. (1992) have stated that the volume of sediment available for aeolian transport on the beaches is modulated by the flux of suspended sediment load from the fluvial to the littoral system. Therefore, an upper limit of sediment available for aeolian transport can be estimated based on the fluvial suspended sediment supplied by the Rio Grande de Nazca. The available river discharge data for the years 1975–2007 (Junta de Usuarios Palpa, 2007) are multiplied with the suspended sediment concentration of two grab samples taken in 2005 during average discharge conditions. As these two samples cannot be considered representative, a range from 50% of the lower to 200% of the higher measured suspended sediment concentration is assumed to represent the range which includes the long-term average value.

Table 1
Dune volume and maximum sand thickness of the Dunas Pampa Blanca derived from ASTER and SRTM DEM.

	Volume	Maximum thickness
ASTER DEM	3.42 km^3	233 m
SRTM DEM	3.44 km^3	215 m

Antiquity of topographic conditions

Favourable conditions for aeolian accumulation in the lee of Cerro Machocoyungo were created by uplift of the Cordillera de la Costa. According to Hsu (1992), the section of the Peruvian coastal desert in the vicinity to the mouth of the Rio Grande de Nazca has been under the influence of the oceanic Nazca Ridge for ca. 1 Ma. However, using the more recently published lower data on plate convergence rate and associated migration of the Nazca Ridge relative to the coast of South America (Norabuena et al., 1998; Hampel, 2002), the area has been affected by uplift for almost 2 Ma. The lower plate convergence rate also explains the discrepancies between observed (ca. 0.5 m ka^{-1}) and modelled (ca. 0.7–0.9 m ka^{-1}) coastal uplift rates (cf. Hsu, 1992; Ortlieb and Macharé, 1990).

To estimate the antiquity of the topographic conditions which allowed the accumulation of the terminal dune field Dunas Pampa Blanca in the lee of the Cordillera de la Costa (Cerro Machocoyungo), the observed coastal uplift rate of ~0.5 m a^{-1} (Hsu, 1992) was applied to the Cordillera de la Costa (Fig. 5). This approach is based on the assumption that the present elevation difference between the lowest pass of the aeolian transport corridor crossing the Cordillera de la Costa and the area of sand deposition is both necessary and sufficient to create wind shadow conditions allowing terminal dune accumulation. The present mean and maximum height of the Dunas Pampa Blanca are used to derive two age estimates.

Results

Terminal dune field volume

From the calculations based on the ASTER and the SRTM DEMs, similar volumes of the Dunas Pampa Blanca of 3.43 km^3 are derived (Table 1). Mean maximum sand thickness is 224 m; average sand thickness is 57 m. Relative error between results derived from ASTER and SRTM is 0.3% (0.01 km^3) for dune volume and 4.0% (9 m) for maximum sand thickness. Figure 6 shows the distribution of sand thickness in the Dunas Pampa Blanca.

Aeolian transport

Dune migration rates are summarised in Table 2. The dune migration rate in the aeolian transport corridor feeding the Dunas Pampa Blanca was 1.28 ± 0.15 m a^{-1} (SD = 0.82 m a^{-1}) for the 29-year period from 1974 to 2003. This is in general agreement with dune migration rates for the shorter periods with even the lowest (0.95 ± 0.33 m a^{-1}, SD = 1.80 m a^{-1}, for the period 1990–2003) and highest

(1.98 ± 0.27 m a^{-1}, SD = 1.50 m a^{-1}, for the period 1974–1990) results overlapping within one standard deviation. The independent determination of dune migration for sequential as well as overlapping time windows thus delivered consistent results. For all time windows, dune migration vectors lie in the north-western quadrant. Taking into account the direction of dune migration, the results for the periods 2000–2003 (43°), 1974–2000 (58°) and 1974–2003 (67°) agree best with the dune migration direction of 31–54° derived manually from the 2003 Quickbird image while the results for the periods 1974–1990 (11°) and 1990–2003 (84°) – which also resulted in the highest and lowest dune migration rates, respectively – are least compatible with the true direction of dune migration. The dune migration rates for the periods 1974–2000 (1.42 ± 0.17 m a^{-1}, SD = 0.95 m a^{-1}), 2000–2003 (1.41 ± 0.50 m a^{-1}, SD = 2.72 m a^{-1}) and 1974–2003 (1.28 ± 0.15 m a^{-1}, SD = 0.82 m a^{-1}) are therefore considered to provide the most reliable results. These dune migration rates are statistically identical at a confidence level of 99%. The data therefore indicate that dune migration rates have been similar over these time windows.

Average dune height determined in the 2003 Quickbird image from the average dune slip face lengths is 6.73 m. In combination with the average dune height, the data on dune displacement allow the volumetric calculation of dune migration. Sand transport by dune migration in the transect under investigation was $4.9 \times 10^4 \pm 5.7 \times 10^3$ m^3 a^{-1} (SD = 3.1×10^4 m^3 a^{-1}) in the period 1974–2003. As this approach only captures sand transport in migrating dunes and ignores transport in suspension and streamers, this is the minimum sand transport rate towards the erg under recent conditions of sand supply and wind regime.

Under the hypothetical assumption that recent conditions of aeolian sediment supply and transport are representative for the Quaternary (i.e. implying climatic stability with regard to all factors influencing sediment supply and transport), the volume of the Dunas Pampa Blanca would thus have accumulated within 70 ± 8 ka. This has to be considered a *maximum age* because it is based on a minimum sand transport estimate.

Limitation of sediment supply

According to the available river discharge data for the period 1975–2007 (Junta de Usuarios Palpa, 2007), mean annual discharge is $3.05 \times 10^8 \pm 1.07 \times 10^8$ m^3 a^{-1} (SD = 8.52×10^7 m^3 a^{-1}). The concentration of suspended sediment measured in two grab samples was 3.0 and 6.6 kg m^{-3}, respectively. It is assumed that a range from 50% of the minimum to 200% of the maximum measured value (i.e. 1.5–13.2 kg m^{-3}) includes the plausible long-term average sediment concentration. The fluvial suspended sediment delivery by the Rio Grande de Nazca is thus estimated to be between 3.0×10^8 and 5.4×10^9 kg a^{-1} (between 2.3×10^5 and 4.2×10^6 m^3 a^{-1} at 1300 kg m^{-3}). However, comparison of the grain size distributions of suspended fluvial sediment in the Rio Grande de Nazca (poorly sorted sandy silt) with the aeolian sediment in the Dunas Pampa Blanca (well-sorted fine to medium sand) indicates that only a limited grain size fraction (~20%) is incorporated in the dunes. Under this limitation, the Rio Grande supplies between 4.6×10^4 and 8.4×10^5 m^3 a^{-1} of sediment for potential aeolian transport. As the sediment transfer efficiency from the fluvial through the littoral to the aeolian system is an unknown fraction of 100%, this represents a maximum estimate for the sediment supply to the aeolian system under recent conditions. Dividing the volume of the terminal Dunas Pampa Blanca by this rate therefore provides a *minimum age* constraint for the Dunas Pampa Blanca of 4–75 ka (99% confidence interval).

Antiquity of topographic conditions

Dune field accumulation can only have commenced much later than the begin of uplift at ca. 2 Ma, because during the initial stages of uplift the Cordillera de la Costa was a suboceanic feature (Hsu, 1992). After subaerial exposure, suitable topographic conditions for the accumulation of the terminal dune field – i.e., the creation of a topographic lee situation downwind of the Cordillera de la Costa – required further uplift. At present, the maximum height of the Dunas Pampa Blanca (647 m according to the SRTM data) is 38 m lower than the height of the lowest pass where the aeolian transport corridor crosses the Cordillera de la Costa (685 m). The mean height of the Dunas Pampa Blanca (471 m according to the SRTM data) is 214 m below the pass height. These height differences between the lowest pass where the aeolian transport corridor crosses the Cordillera de la Costa and (a) the height of the highest dune and (b) the mean height of the Dunas Pampa Blanca characterise the wind shadow conditions under which aeolian accumulation takes place. Comparison with the topographic situation of the Dunas Usaca (ca. 30 km to the south-east) and the Ica dune field (ca. 60 km to the north-west) indicates that these dune fields are located in wind shadows created by elevation differences of 120–340 m.

Assuming that the wind shadow conditions created by the uplift of the Cordillera de la Costa are both necessary and sufficient to allow the accumulation of aeolian sand in the lee of Cerro Machocoyungo, the age of topographic conditions favourable for dune field creation can be constrained using the uplift rate. Thus, by dividing the average (57 m) and maximum (224 m) sand thickness of the Dunas Pampa Blanca by the coastal uplift rate of 0.5 m a^{-1} (Hsu, 1992), the potential age of the dune field based on topographic conditions can be constrained to 110–450 ka. However, while uplift primarily affects the Cordillera de la Costa, to an unknown but lower extent it also affects the location of the Dunas Pampa Blanca. The age of 110–450 ka therefore represents a *minimum age* for the creation of topographic conditions favourable for aeolian accumulation.

Discussion

Regional context of dune migration rates

At 1.28 ± 0.15 m a^{-1}, the migration rate of transverse dunes in the aeolian transport corridor feeding the Dunas Pampa Blanca is much lower than that found by Gay (1999) for migrating barchans in the Pampa de Jaguay, approx. 90 km to the south-east (10–60 m a^{-1}). However, this difference can be attributed to a number of independent factors. Under a given wind and sediment supply regime, migration rates of transverse and barchan dunes depend on dune type (with barchans having the fastest migration rates) and are inversely related to dune size. The dunes in the aeolian transport corridor feeding the Dunas Pampa Blanca are coalescing transverse dunes while the dunes studied by Gay (1999) are generally well-separated barchans of varying size. While empirical relationships between barchan size and migration rate have been established by Gay (1999), no comparable studies exist for coalescing transverse dunes. Furthermore, even though both areas are located in the coastal desert of southern Peru, they are not necessarily subject to the same wind regime. The Pampa de Jaguay dune swarm studied by Gay (1999) is subject to only weakly topographically modified south-east trade winds, but dune migration towards the Dunas Pampa Blanca shows strong topographic control over the wind direction (and hence presumably also over wind strength): winds are from south at the coast and shift to south-west near the terminal dune field, departing by 90° from the south-east trade winds (cf. Gay, 2005). The two areas further differ in representing a transport corridor along a topographic depression in the case of the Pampa de Jaguay and a transport corridor over a topographic high (Cerro Machocoyungo) in the case of the dunes migrating towards the Dunas Pampa Blanca. Sedimentological differences between the dunes in the two areas may potentially also contribute to diverging migration rates. The low dune-migration rate found here therefore is not considered unusual.

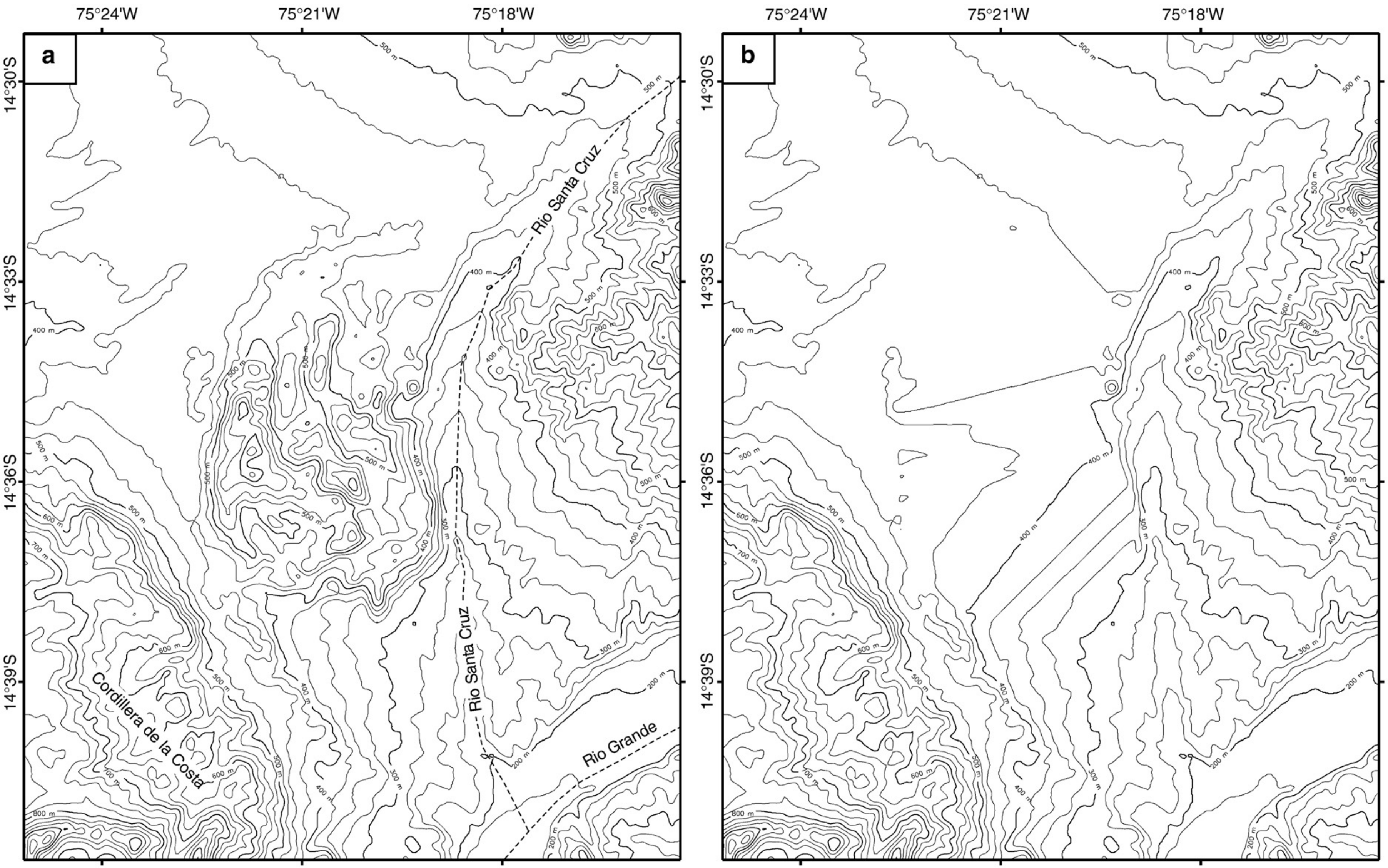

Figure 6. Distribution of sand thickness in the Dunas Pampa Blanca derived from SRTM DEM and interpolated basal topography. (a) SRTM DEM with Dunas Pampa Blanca, (b) SRTM DEM with interpolated basal topography in place of the Dunas Pampa Blanca, (c) sand thickness of the Dunas Pampa Blanca. Contour interval is 25 m.

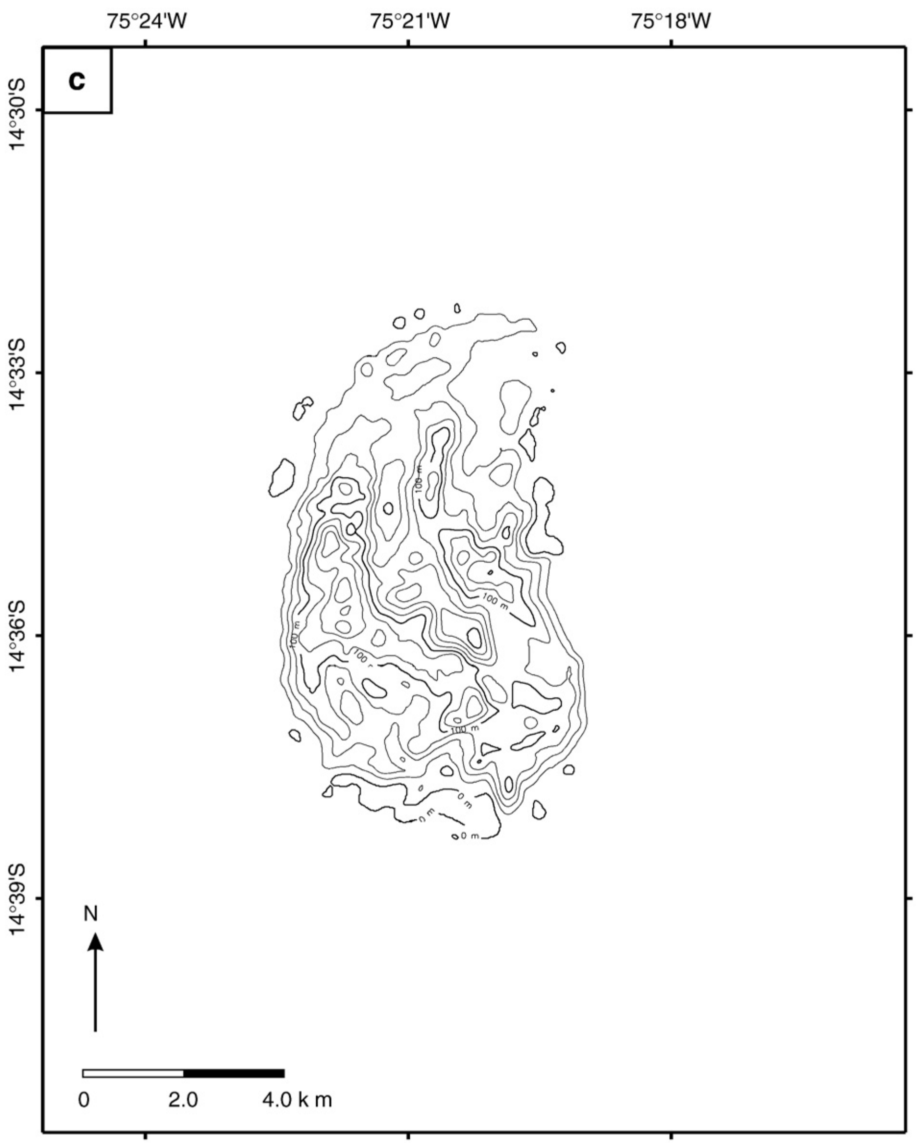

Figure 6 (*continued*).

Paleoenvironmental implications

The sediment supply, transport and storage calculations and the derived age constraints were based on the hypothesis of Quaternary climatic stability with regard to fluvial and aeolian processes and in particular on the hypothesis that present conditions might be representative for the Quaternary. Comparison of the different aeolian transport and dune field age estimates allows these hypotheses to be tested.

Table 3 summarises the age estimates for the Dunas Pampa Blanca. From the minimum sand transport rate and the total volume of the

Table 2
Results of the cross-correlation approach to dune migration rates.

			1974–1990		1990–2000		2000–2003		1990–2003		1974–2000		1974–2003	
			Mean	SD	Mean	SD	Mean	SD	Mean	SD	Mean	SD	Mean	SD
Cross-correlation	Dune-free areas	*X* shift [m]	−16.51	12.60	20.90	5.66	−10.71	2.34	12.30	8.87	−1.84	9.16	−11.34	8.87
		Y shift [m]	−3.15	10.60	1.48	9.41	−12.87	2.82	−15.74	19.03	−7.70	7.80	−21.97	9.63
		n (outliers)	200 (10)		200 (9)		200 (0)		200 (5)		200 (0)		200 (0)	
	Dune-covered areas	*X* shift [m]	−10.46	12.09	33.87	1.67	−7.93	2.47	24.45	2.86	29.31	14.29	22.57	15.24
		Y shift [m]	−34.19	12.41	−1.53	3.98	−15.85	6.46	−17.08	9.53	−27.54	16.15	−36.60	12.62
		n (Outliers)	300 (7)		300 (0)		300 (0)		300 (0)		300 (0)		300 (7)	
	Difference	*X* [m]	6.05	17.46	12.97	5.90	2.78	3.40	12.15	9.32	31.15	16.98	33.91	17.63
		Y [m]	−31.04	16.32	−3.01	10.22	−2.99	7.05	−1.34	21.28	−19.84	17.93	−14.63	15.87
Dune migration		Total [m]	31.63	23.90	13.32	11.80	4.08	7.83	12.22	23.24	36.93	24.69	36.93	23.72
		Annual rate [m a^{-1}]	1.98	1.50	1.33	1.18	1.41	2.72	0.95	1.80	1.42	0.95	1.28	0.82
		99% Confidence interval [m a^{-1}]	1.98 ± 0.27		1.33 ± 0.22		1.41 ± 0.50		0.95 ± 0.33		1.42 ± 0.17		1.28 ± 0.15	
		Direction [°]	11		77		43		84		58		67	

https://doi.org/10.1016/j.yqres.2009.02.002 Published online by Cambridge University Press

Table 3
Comparison of age estimates for the accumulation of the Dunas Pampa Blanca.

Age determination based on	Age
Transverse dune migration	$\leq 70 \pm 8$ ka
Fluvial sediment delivery	≥ 4–75 ka
Favourable topographic conditions	≥ 110–450 ka

Dunas Pampa Blanca it follows that under present sand transport conditions the *maximum age* of the dune field is 70 ± 8 ka. While this is compatible with the estimates derived from the sediment supply calculations which indicate a *minimum age* of 4–75 ka under the assumption of a long-term persistence of recent conditions, it is at odds with the *minimum age* of 110–450 ka deduced from the tectonic/topographic considerations. This indicates that, based on the age of favourable wind shadow conditions in the lee of Cerro Machocoyungo, dune field accumulation could have occurred over a time span *at least* 1.6–6.4 times longer than that suggested by the observation of present-day sediment supply.

If present conditions of sand supply and transport were representative for the late Quaternary, a much larger volume of sand should have accumulated in the Dunas Pampa Blanca. Present conditions can therefore not be considered representative for the Quaternary. The discrepancy between the maximum age deduced from sand transport calculations and the minimum age from tectonic/topographic considerations indicates that after the creation of topographic conditions favourable for the formation of the terminal dune field, average sand accumulation rate was on average *less than* 14–71% of the present rate. This could be explained by (a) phases of reduced sediment availability, (b) phases of reduced sediment transport or (c) phases of dune field erosion. All of these explanations require climatic changes. While (a) implies changes in sediment delivery by the Rio Grande de Nazca, (b) points to possible changes in wind strength or direction and (c) implies either changes in wind strength or direction or, alternatively, considerable local precipitation in the coastal desert.

Comparison of the recent aeolian transport rate (at least $4.9 \times 10^4 \pm 5.7 \times 10^3$ m^3 a^{-1}) with the recent sediment supply from the fluvial system (at most 4.6×10^4 – 8.4×10^5 m^3 a^{-1}) shows that these two ranges are compatible, i.e. the aeolian transport rate is near the lower limit of the rate of sediment supply from the fluvial system. If sediment supply and transport had occurred at constant rates during the late Quaternary, this could be interpreted as suggesting a sediment transfer efficiency from the fluvial through the littoral to the aeolian system between 5 and 100%. However, as aeolian transport by dune migration was observed ~20 km inland from the coast, the time lag caused by the migration time from the coast to the present dune locations has to be taken into account. Given the dune migration rate of 1.28 ± 0.15 m a^{-1}, this time lag may be as much as 14–18 ka. Taking into account that over much of the distance from the coast sand transport is achieved by faster-migrating barchans rather than by slower transverse dunes, this is a maximum time lag estimate. The difference between the two rates may thus be due to temporal changes in sediment supply. Such temporal changes in sediment supply at the source of aeolian transport were found for a barchan dune swarm in the Pampa de Jaguay, ~90 km south-east of the Dunas Pampa Blanca. There, reconstructed aeolian sediment supply to the aeolian system was found to have been low during the past 300 a compared to average middle to late Holocene conditions (Hesse, 2008).

The fine fraction (mainly silt) of aeolian sediment is transported in suspension rather than in migrating dunes. This suspended aeolian sediment is transported further inland and may accumulate as desert loess at the foot of the Cordillera Occidental or be incorporated into vesicular layers under bajada desert pavements (Noller, 1993; McFadden et al., 1998). However, at present no desert loess accumulation takes place (Eitel et al., 2005; Hesse and Baade 2007). This cannot be attributed to lacking supply from the fluvial into the aeolian system as grain size distributions of suspended fluvial sediment show that it is rich in silt. Thus, while the results of this study indicate that recent aeolian transport is *at least* 1.6–6.4 times higher than the average for the late Quaternary, the lack of recent desert loess accumulation in areas with fossil desert loess cover implies that there must have been times of even higher aeolian fluxes. According to the Global Seafloor Topography (Smith and Sandwell, 1997) as well as marine bathymetry profiles (National Geophysical Data Center, 2004), the shelf in the vicinity of the mouth of the Rio Grande de Nazca has a width of approximately 15 km with a slope of ≤ 1%. Under conditions prevailing during glaciations, this shelf area with a present-day water depth of ≤ 130 m was exposed to deflation. In combination with stronger winds due to increased latitudinal temperature contrasts, higher rates of aeolian transport should be expected during Glacial periods (Garleff et al., 1991; Lancaster, 1994b). To achieve the low average rate of aeolian accumulation implied by the volume and potential age of the Dunas Pampa Blanca, periods of greatly reduced aeolian flux or (partial) erosion of the Dunas Pampa Blanca therefore have to be postulated. While discrete phases of aeolian activity have been reconstructed for the Thar Desert of India (e.g. Thomas, 1999), comparable studies are so far not available for the coastal desert of Peru. Given the results and implications discussed here, investigations regarding temporal changes in dune field accumulation in Peru are necessary to quantify the temporal variability of aeolian transport and accumulation.

Conclusions

Observations of aeolian sediment transport in migrating transverse dunes as well as fluvial sediment supply constrain the age of aeolian accumulation of the Dunas Pampa Blanca to a *minimum age* of 4–75 ka and a *maximum age* of 70 ± 8 ka under the assumption that recent conditions are representative for the late Quaternary. These constraints are not compatible with the *minimum age* 110–450 ka for topographic conditions favourable for aeolian accumulation in the lee of Cerro Machocoyungo. The hypothesis of late Quaternary stability with conditions similar to the present therefore has to be rejected. Recent aeolian sediment transport rates are not representative and are *at least* 1.6–6.4 higher than average for the late Quaternary.

The present study shows that changes in net sand accumulation must have taken place during the late Quaternary. However, it cannot deliver information regarding the causes underlying the discrepancies between the estimated minimum and maximum ages of the Dunas Pampa Blanca. These discrepancies will have to be attributed to, either individually or in combination, temporal changes in sediment availability and transport as well as possible periods of erosion of the Dunas Pampa Blanca. All of these mechanisms imply climatic changes in the coastal desert. These changes are likely recorded in the stratigraphy of the Dunas Pampa Blanca. With an estimated age depth of between 70 ± 8 ka and perhaps more than 450 ka recorded in the Dunas Pampa Blanca, further research has the potential to contribute significantly to the reconstruction of the presently poorly understood climatic history of the Peruvian coastal desert.

References

Alpers, C.N., Brimhall, G.H., 1988. Middle Miocene climatic change in the Atacama Desert, northern Chile: evidence for supergene mineralization at La Escondida. Bulletin of the Geological Society of America 100 (10), 1640–1656.

Arancibia, G., Matthews, S., de Arce, C.P., 2005. K–Ar and ^{40}Ar/^{39}Ar ages from supergene minerals in northern Chile: prevalence of humid climate and tectonic uplift until the Upper Miocene in the Atacama Desert. 6th International Symposium on Andean Geodynamics (ISAG 2005, Barcelona), Extended Abstracts, pp. 50–52.

Barber, R.T., Chavez, F.P., 1983. Biological consequences of El Niño. Science 222, 1203–1210.

Besler, H., 2002. The Great Sand Sea (Egypt) during the Late Pleistocene and the Holocene. Zeitschrift für Geomorphologie 127 (N.F. Suppl.-Bd), 1–19.

Bourke, M.C., Balme, M., Beyer, R.A., Williams, K.K., Zimbelman, J., 2006. A comparison of methods used to estimate the height of sand dunes on Mars. Geomorphology 81, 440–452.

Cane, M.A., 1983. Oceanographic events during El Niño. Science 222, 1189–1195.

Caviedes, C., 1973. A climatic profile of the North Chilean Desert at latitude 20°S. In: Amiran, D.H.K., Wilson, A.W. (Eds.), Coastal deserts, their natural and human environments. University of Arizona Press, Tuscon, pp. 115–121.

Caviedes, C.N., 1984. Geography and the lessons from El Niño. Professional Geographer 36 (4), 428–436.

Clarke, J.D.A., 2006. Antiquity of aridity in the Chilean Atacama Desert. Geomorphology 73, 101–114.

de Abreu, M.L., Bannon, P.R., 1993. Dynamics of the South American coastal desert. Journal of the Atmospheric Sciences 50 (17), 2952–2964.

DigitalGlobe, Inc., 2003. Quickbird image, catalogue ID 1010010001 B7C001, acquisition: March 03, 2003. accessible through Google Earth (earth.google.com).

Eitel, B., Hecht, S., Mächtle, B., Schukraft, G., Kadereit, A., Wagner, G.A., Kromer, B., Unkel, I., Reindel, M., 2005. Geoarchaeological evidence from desert loess in the Nazca–Palpa region, southern Peru: palaeoenvironmental changes and their impact on pre-Columbian cultures. Archaeometry 47 (1), 137–158.

Evenstar, L., Hartley, A., Rice, C., Stuart, F., Mather, A., Chong, G., 2005. Miocene–Pliocene climate change in the Peru–Chile Desert. 6th International Symposium on Andean Geodynamics (ISAG 2005, Barcelona), Extended Abstracts, pp. 258–260.

Finkel, H.J., 1959. The barchans of southern Peru. Journal of Geology 67, 614–647.

Forman, S.L., Oglesby, R., Webb, R.S., 2001. Temporal and spatial patterns of Holocene dune activity on the Great Plains of North America: megadroughts and climate links. Glob. Planet. Change. 29, 1–29.

Garleff, K., Schäbitz, F., Stingle, H., Veit, H., 1991. Jungquartäre Landschaftsentwicklung und Klimageschichte beiderseits der ariden Diagonale Südamerikas. Bamberger Geographische Schriften 11, 359–394.

Gay, P., 1962. Origen, distribución y movimiento de las arenas eólicas en al área de Yauca a Palpa. Boletín de la Sociedad Geológica del Perú 37, 37–58.

Gay Jr, S.P., 1999. Observations regarding the movement of barchan sand dunes in the Nazca to Tanaca area of southern Peru. Geomorphology 27, 279–293.

Gay Jr, S.P., 2005. Blowing sand and surface winds in the Pisco to Chala area, southern Peru. Journal of Arid Environments 61 (1), 101–117.

GLCF (Global Land Cover Facility), 2004. Landsat MSS EarthSat-Orthorectified satellite image, scene p006r7019740430. Global Land Cover Facility, University of Maryland. http://glcf.umiacs.umd.edu [28.02.2004].

Grosjean, M., Cartajena, I., Geyh, M.A., Núñez, L., 2003. From proxy data to paleoclimate interpretation: the mid-Holocene paradox of the Atacama Desert, northern Chile. Palaeogeography, Palaeoclimatology, Palaeoecology 194, 247–258.

Hampel, A., 2002. The migration history of the Nazca Ridge along the Peruvian active margin: a re-evaluation. Earth and Planetary Science Letters 203, 665–679.

Hesse, R., 2008. Do swarms of migrating barchan dunes record paleoenvironmental changes? — a case study spanning the middle to late Holocene in the Pampa de Jaguay, southern Peru. Geomorphology, doi:10.1016/j.geomorph.2008.08.006.

Hesse, R., Baade, J., 2007. Palaeoenvironmental changes in the Nazca–Palpa region, southern Peru — alternative interpretations of geoarchaeological evidence: a comment on Eitel et al. (2005) in Archaeometry, Vol. 47(1). Archaeometry 49 (3), 595–602.

Houston, J., Hartley, A.J., 2003. The central Andean west-slope rainshadow and its potential contribution to the origin of hyper-aridity in the Atacama Desert. International Journal of Climatology 23, 1453–1464.

Hsu, J.T., 1992. Quaternary uplift of the Peruvian coast related to the subduction of the Nazca Ridge: 13.5 to 15.6 degrees south latitude. Quaternary International 15/16, 87–97.

Junta de Usuarios Palpa, 2007. Daily discharge data for the drainage basin of the Rio Grande de Nazca 1975–2007. unpublished data.

Lancaster, N., 1994a. Controls on aeolian activity: some new perspectives from the Kelso Dunes, Mojave Desert, California. Journal of Arid Environments 27, 113–125.

Lancaster, N., 1994b. Dune morphology and dynamics. In: Abrahams, A.D., Parsons, A.J. (Eds.), Geomorphology of desert environments. Chapman & Hall, London, pp. 474–505.

Lettau, K., Lettau, H., 1969. Bulk transport of sand by the barchans of the Pampa de La Loya in southern Peru. Zeitschrift für Geomorphologie 13, 182–195.

Lewis, A.J., Henderson, F.M., Holcomb, D.W., 1998. Radar fundamentals: the geoscience perspective, In: Henderson, F.M., Lewis, A.J. (Eds.), Manual of Remote Sensing., Vol. 2. Principles and applications of imaging radars, 3rd ed. Wiley, New York, pp. 131–180.

Macharé, J., Veliz, Y., Ortlieb, L., Dumont, J.-F., 1990. A review of recent paleoclimatic studies in Peru. Quaternary of South America and Antarctic Peninsula 8, 157–176.

Mahan, S.A., Miller, D.M., Manges, C.M., Yount, J.C., 2007. Late Quaternary stratigraphy and luminescence geochronology of the northeastern Mojave Desert. Quaternary International 166, 61–78.

McFadden, L.D., McDonald, E.V., Wells, S.G., Anderson, K., Quade, J., Forman, S.L., 1998. The vesicular layer and carbonate collars of desert soils and pavements: formation, age and relation to climate change. Geomorphology 24 (2–3), 101–145.

McGowen, H.A., Petherick, L.M., Kamber, B.S., 2008. Aeolian sedimentation and climate variability during the late Quaternary in southeast Queensland, Australia. Palaeogeogr. Palaeoclimatol. Palaeoecol. 265, 171–181.

Messerli, B., Grosjean, M., Graf, K., Schotterer, U., Schreier, H., Vuille, M., 1992. Die Veränderungen von Klima und Umwelt in der Region Atacama (Nordchile) seit der letzten Kaltzeit. Erdkunde 46, 257–272.

Messerli, B., Grosjean, M., Bonani, G., Bürgi, A., Geyh, M.A., Graf, K., Ramseyer, K., Romero, H., Schotterer, U., Schreier, H., Vuille, M., 1993. Climate change and natural resource dynamics of the Atacama Altiplano during the last 18 000 years: a preliminary synthesis. Mt. Res. Dev. 13 (2), 117–127.

Moseley, M.E., Wagner, D., Richardson III, J.B., 1992. Space shuttle imagery of recent catastrophic change along the arid Andean coast. In: Johnson, L.L., Stright, M. (Eds.), Paleoshorelines and prehistory: an investigation of method. CRC Press, Boca Raton, pp. 215–235.

NASA, 2005. Landsat composite images. NASA Earth Science Applications Directorate. https://zulu.ssc.nasa.gov/mrsid/mrsid.pl [26 January 2005].

NASA, 2006a. SRTM version 2. ftp://e0srp01u.ecs.nasa.gov/srtm/version2 [13 July 2006].

NASA, 2006b. ASTER-DEM, data set ID: ASTER_DEM20041019164300.hdf. Land Processes Distributed Active Archive Center. http://lpdaac.usgs.gov/support/list.php[24 January 2006].

National Geophysical Data Center, 2004. Bathymetric surveys C2306, YAQ7306, 8503, FD774BMV and PIQR04WT. Marine trackline geophysics and hydrographic surveys databases. http://www.ngdc.noaa.gov/mgg/gdas/gd_sys.html [06 May 2004].

Noller, J.S., 1993. Late Cenozoic stratigraphy and soil geomorphology of the Peruvian Desert, 3° to 18°S: a long-term record of hyperaridity and El Niño. PhD thesis, University of Colorado, Boulder.

Norabuena, E., Leffler-Griffin, L., Mao, A., Dixon, T., Stein, S., Sacks, I.S., Ocola, L., Ellis, M., 1998. Space geodetic observations of Nazca–South America convergence across the central Andes. Science 279, 358–362.

Oberlander, T.M., 1994. Global deserts: a geomorphic comparison. In: Abrahams, A.D., Parsons, A.J. (Eds.), Geomorphology of desert environments. Chapman and Hall, London, pp. 13–36.

ONERN (Oficina Nacional De Evaluación De Recursos Naturales), 1971. Inventario, evaluación y uso racional de los recursos naturales de la costa: cuenca de Río Grande (Nazca), vol. I + II. ONERN: Lima.

Ortlieb, L., Macharé, J., 1990. Geocronología y morfostratigrafía de terrazas del Pleistoceno superior: El caso de San Juan–Marcona, Peru. Boletín de la Sociedad Geológica del Perú 81, 87–106.

Prohaska, F.J., 1973. New evidence on the climatic controls along the Peruvian coast. In: Amiran, D.H.K., Wilson, A.W. (Eds.), Coastal deserts, their natural and human environments. University of Arizona Press, Tuscon, pp. 91–107.

Radies, D., Preusser, F., Matter, A., Mange, M., 2004. Eustatic and climatic controls on the development of the Wahiba Sand Sea, Sultanate of Oman. Sedimentology 51, 1359–1385.

Rech, J.A., Currie, B.S., Cowan, A., Michalski, G., 2006. Mid-Miocene nitrate paleosols from the Atacama Desert: implications for the antiquity of the Atacama Desert. 18th World Congress of Soil Science, July 9–15, 2006, Philadelphia, Pennsylvania, USA.

Sébrier, M., Macharé, J., 1980. Observaciones acerca del Cuaternario de la costa del Perú central. Bulletin de l'Institut Français d'Études Andines 9 (1–2), 5–22.

Singhvi, A.K., Kar, A., 2004. The aeolian sedimentation record of the Thar Desert. Proceedings of the Indian Academy of Sciences (Earth and Planetary Sciences) 113 (3), 371–401.

Smith, W.H.F., Sandwell, D.T., 1997. Global seafloor topography from satellite altimetry and ship depth soundings. Science 277, 1956–1962.

Sun, P., 2006. Outlier detection in high dimensional, spatial and sequential data sets. PhD thesis, University of Sydney.

Thomas, J.V., 1999. Late Pleistocene–Holocene history of aeolian accumulation in the Thar Desert. Zeitschrift für Geomorphologie 116 (N.F. Suppl.-Bd), 181–194.

Unkel, I., 2006. AMS-^{14}C-Analysen zur Rekonstruktion der Landschafts- und Kulturgeschichte in der Region Palpa (S-Peru). Dissertation, University Heidelberg.

Wang, X., Dong, Z., Liu, L., Qu, J., 2004. Sand sea activity and interactions with climatic parameters in the Taklimakan Sand Sea, China. Journal of Arid Environments 57, 85–98.

Wasson, R.J., Rajaguru, S.N., Misra, V.N., Agrawal, D.P., Dhir, R.P., Singhvy, A.K., Kameswara Rao, K., 1983. Geomorphology, Late Quaternary stratigraphy and paleoclimatology of the Thar dunefield. Zeitschrift für Geomorphologie 45 (N.F. Suppl.-Bd), 117–151.

Weischet, W., 1966. Zur Klimatologie der Nordchilenischen Wüste. Meteorologische Rundschau 19 (1), 1–7.

Weischet, W., 1996. Regionale Klimatololgie. Teil 1: Die Neue Welt. B.G. Teubner: Stuttgart.

Wernstedt, J., 1989. Experimentelle Prozeβanalyse. Verlag Technik, Berlin.

Wolfe, S.A., Paulen, R.C., Smith, I.R., Lamothe, M., 2007. Age and paleoenvironmental significance of Late Wisconsinan dune fields in the Mount Watt and Fontas River map areas, northern Alberta and British Columbia. Geological Society of Canada Current Research 2007-B4, (10 pp).

Zárate, M., Blasi, A., 1993. Late Pleistocene–Holocene eolian deposits of the southern Buenos Aires province, Argentina: a preliminary model. Quaternary International 17, 15–20.